SUPPLEMENTAL MATERIAL

Data S1. Statistical methods

We used the following to denote an indicator function and a ramp function.

$[c] = 1$ if subject is in group c, 0 otherwise; $(x)_+ = x$ if $x > 0$, 0 otherwise

We also denoted QRS duration and pulmonary regurgitation fraction by QRS and PRF, respectively.

1 Unadjusted regression equations

The estimated unadjusted regression equations are

$$
\begin{aligned}
\text{E(Peak VO}_2) = {} & 147.8166 - 0.97761\,\text{QRS} - 1.86186\,\text{PRF} + \\
& 0.00041\,(\text{QRS}-96)_+^3 - 0.00195\,(\text{QRS}-128)_+^3 + 0.00307\,(\text{QRS}-144)_+^3 - \\
& 0.00159\,(\text{QRS}-152)_+^3 + 5.14479\times10^{-5}\,(\text{QRS}-170)_+^3 - \\
& 0.00179\,(\text{PRF}-5)_+^3 + 0.02694\,(\text{PRF}-31)_+^3 - 0.08738\,(\text{PRF}-40)_+^3 + \\
& 0.09876\,(\text{PRF}-47)_+^3 - 0.03653\,(\text{PRF}-54)_+^3 + \\
& \text{QRS}\,\Big\{0.01582\,\text{PRF} + 1.61583\times10^{-5}\,(\text{PRF}-5)_+^3 - 0.00022\,(\text{PRF}-31)_+^3 + \\
& \quad 0.00066\,(\text{PRF}-40)_+^3 - 0.00072\,(\text{PRF}-47)_+^3 + 0.00026\,(\text{PRF}-54)_+^3\Big\} + \\
& \text{PRF}\,\Big\{7.08476\times10^{-6}\,(\text{QRS}-96)_+^3 - 9.44531\times10^{-5}\,(\text{QRS}-128)_+^3 + \\
& \quad 0.00029\,(\text{QRS}-144)_+^3 - 0.00023\,(\text{QRS}-152)_+^3 + 2.44597\times10^{-5}\,(\text{QRS}-170)_+^3\Big\}
\end{aligned}
$$

$$
\begin{aligned}
\text{E(Percent predicted VO}_2) = {} & 246.9357 - 1.35484\,\text{QRS} - 2.662\,\text{PRF} + \\
& 0.00045\,(\text{QRS}-96)_+^3 - 0.00159\,(\text{QRS}-128)_+^3 + 0.00128\,(\text{QRS}-144)_+^3 + \\
& 6.66333\times10^{-6}\,(\text{QRS}-152)_+^3 - 0.00014\,(\text{QRS}-170)_+^3 - \\
& 0.0026\,(\text{PRF}-5)_+^3 + 0.04865\,(\text{PRF}-31)_+^3 - 0.17193\,(\text{PRF}-40)_+^3 + \\
& 0.2022\,(\text{PRF}-47)_+^3 - 0.07633\,(\text{PRF}-54)_+^3 + \\
& \text{QRS}\,\Big\{0.01664\text{PRF} + 2.7652\times10^{-5}(\text{PRF}-5)_+^3 - 0.00042(\text{PRF}-31)_+^3 + \\
& \quad 0.00136\,(\text{PRF}-40)_+^3 - 0.00153\,(\text{PRF}-47)_+^3 + 0.00057\,(\text{PRF}-54)_+^3\Big\} + \\
& \text{PRF}\,\Big\{1.21243\times10^{-5}\,(\text{QRS}-96)_+^3 - 0.00018\,(\text{QRS}-128)_+^3 + 6\times10^{-4}\,(\text{QRS}-144)_+^3 - \\
& \quad 0.00048\,(\text{QRS}-152)_+^3 + 5.70184\times10^{-5}\,(\text{QRS}-170)_+^3\Big\}
\end{aligned}
$$

$$
\begin{aligned}
\text{E(RV EF)} = {} & 66.36041 - 0.20258\,\text{QRS} + 3.15599\,\text{PRF} + \\
& 0.00014\,(\text{QRS}-96)_+^3 - 0.00079\,(\text{QRS}-128)_+^3 + 4.70158\times10^{-5}\,(\text{QRS}-144)_+^3 +
\end{aligned}
$$

$$
\begin{aligned}
&0.00117\,(\mathrm{QRS}-152)_+^3 - 0.00058\,(\mathrm{QRS}-170)_+^3 - \\
&0.00347\,(\mathrm{PRF}-5)_+^3 + 0.04447\,(\mathrm{PRF}-31)_+^3 - 0.10589\,(\mathrm{PRF}-40)_+^3 + \\
&0.08992\,(\mathrm{PRF}-47)_+^3 - 0.02504\,(\mathrm{PRF}-54)_+^3 + \\
&\mathrm{QRS}\,\Big\{-0.02244\,\mathrm{PRF} + 2.44557\times10^{-5}\,(\mathrm{PRF}-5)_+^3 - 0.00032\,(\mathrm{PRF}-31)_+^3 + \\
&\qquad 0.00077\,(\mathrm{PRF}-40)_+^3 - 0.00067\,(\mathrm{PRF}-47)_+^3 + 0.00019\,(\mathrm{PRF}-54)_+^3 + \Big\} \\
&\mathrm{PRF}\,\Big\{1.07228\times10^{-5}\,(\mathrm{QRS}-96)_+^3 - 0.00014\,(\mathrm{QRS}-128)_+^3 + 0.00034\,(\mathrm{QRS}-144)_+^3 - \\
&\qquad 0.00021\,(\mathrm{QRS}-152)_+^3 - 1.42996\times10^{-6}\,(\mathrm{QRS}-170)_+^3\Big\}
\end{aligned}
$$

2 Covariate-adjusted regression equations

The estimated covariate-adjusted regression equations are

$$
\begin{aligned}
&\mathrm{E}(\text{Peak } \mathrm{VO_2}) = 174.2491 - 0.56777\,\mathrm{Age} - 4.9794\,\mathrm{BSA} + 4.23814\,[\mathrm{Male}] - \\
&0.10510\,\mathrm{HR\ MRI} - 0.97461\,\mathrm{QRS} - 3.3355\,\mathrm{PRF} + \\
&0.0003\,(\mathrm{QRS}-96)_+^3 - 0.00092\,(\mathrm{QRS}-128)_+^3 + 7.11016\times10^{-5}\,(\mathrm{QRS}-144)_+^3 + \\
&0.00081\,(\mathrm{QRS}-152)_+^3 - 0.00026\,(\mathrm{QRS}-170)_+^3 - \\
&0.00016\,(\mathrm{PRF}-5)_+^3 + 0.01092\,(\mathrm{PRF}-31)_+^3 - 0.05103\,(\mathrm{PRF}-40)_+^3 + \\
&0.06727\,(\mathrm{PRF}-47)_+^3 - 0.027\,(\mathrm{PRF}-54)_+^3 + \\
&\mathrm{QRS}\,\Big\{0.02432\mathrm{PRF} + 5.30983\times10^{-6}(\mathrm{PRF}-5)_+^3 - 0.00011(\mathrm{PRF}-31)_+^3 + \\
&\qquad 0.00042\,(\mathrm{PRF}-40)_+^3 - 0.00052\,(\mathrm{PRF}-47)_+^3 + 0.0002\,(\mathrm{PRF}-54)_+^3\Big\} + \\
&\mathrm{PRF}\,\Big\{2.32814\times10^{-6}\,(\mathrm{QRS}-96)_+^3 - 4.8851\times10^{-5}\,(\mathrm{QRS}-128)_+^3 + 0.00019\,(\mathrm{QRS}-144)_+^3 - \\
&\qquad 0.00016\,(\mathrm{QRS}-152)_+^3 + 2.43571\times10^{-5}\,(\mathrm{QRS}-170)_+^3\Big\}
\end{aligned}
$$

$$
\begin{aligned}
&\mathrm{E}(\text{Percent predicted } \mathrm{VO_2}) = 353.9556 - 1.49809\,\mathrm{Age} - 9.7086\,\mathrm{BSA} + 0.35758[\mathrm{Male}] - \\
&0.187401\,\mathrm{HR\ MRI} - 1.84289\,\mathrm{QRS} - 6.46064\,\mathrm{PRF} + \\
&0.00056\,(\mathrm{QRS}-96)_+^3 - 0.00158\,(\mathrm{QRS}-128)_+^3 - 0.00036\,(\mathrm{QRS}-144)_+^3 + \\
&0.00191\,(\mathrm{QRS}-152)_+^3 - 0.00053\,(\mathrm{QRS}-170)_+^3 - \\
&0.00052\,(\mathrm{PRF}-5)_+^3 + 0.02354\,(\mathrm{PRF}-31)_+^3 - 0.10593\,(\mathrm{PRF}-40)_+^3 + \\
&0.13819\,(\mathrm{PRF}-47)_+^3 - 0.05527\,(\mathrm{PRF}-54)_+^3 + \\
&\mathrm{QRS}\,\Big\{0.0463\,\mathrm{PRF} + 1.29855\times10^{-5}\,(\mathrm{PRF}-5)_+^3 - 0.00024\,(\mathrm{PRF}-31)_+^3 + \\
&\qquad 0.00089\,(\mathrm{PRF}-40)_+^3 - 0.00107\,(\mathrm{PRF}-47)_+^3 + 0.00041\,(\mathrm{PRF}-54)_+^3\Big\} + \\
&\mathrm{PRF}\,\Big\{5.69359\times10^{-6}\,(\mathrm{QRS}-96)_+^3 - 0.00011\,(\mathrm{QRS}-128)_+^3 + 0.00039\,(\mathrm{QRS}-144)_+^3 -
\end{aligned}
$$

$$0.00034\,(\text{QRS}-152)_+^3 + 4.85806\times10^{-5}\,(\text{QRS}-170)_+^3\Big\}$$

$$\begin{aligned}
\text{E(RV EF)} = {} & 115.4021 - 1.06927\,\text{Age} + 3.8795\,\text{BSA} - 0.74171[\text{Male}] - \\
& 0.123603\,\text{HR MRI} - 0.47508\,\text{QRS} + 1.89948\,\text{PRF} + \\
& 0.00026\,(\text{QRS}-96)_+^3 - 0.00149\,(\text{QRS}-128)_+^3 + 0.00158\,(\text{QRS}-144)_+^3 + \\
& 0.00013\,(\text{QRS}-152)_+^3 - 0.00048\,(\text{QRS}-170)_+^3 - \\
& 0.00299\,(\text{PRF}-5)_+^3 + 0.03969\,(\text{PRF}-31)_+^3 - 0.09509\,(\text{PRF}-40)_+^3 + \\
& 0.08067\,(\text{PRF}-47)_+^3 - 0.02229\,(\text{PRF}-54)_+^3 + \\
& \text{QRS}\,\Big\{-0.01212\,\text{PRF} + 2.10403\times10^{-5}\,(\text{PRF}-5)_+^3 - 0.00028\,(\text{PRF}-31)_+^3 + \\
& \qquad 0.00068\,(\text{PRF}-40)_+^3 - 0.00059\,(\text{PRF}-47)_+^3 + 0.00017\,(\text{PRF}-54)_+^3\Big\} + \\
& \text{PRF}\,\Big\{9.22529\times10^{-6}\,(\text{QRS}-96)_+^3 - 0.00012\,(\text{QRS}-128)_+^3 + 0.0003\,(\text{QRS}-144)_+^3 - \\
& \qquad 0.00018\,(\text{QRS}-152)_+^3 - 1.55424\times10^{-6}\,(\text{QRS}-170)_+^3\Big\}
\end{aligned}$$

Data S2. Supplemental Material: Computer modeling

Supplementary Methods

Valve module and Pulmonary Valve Regurgitation

The valve module is used to simulate blood flow across any connection between two cavities or a cavity and a tube in the CircAdapt model where energy losses might occur. Cardiac valves connect cardiac cavities, representing atrio-ventricular valves, or connect cardiac cavities with large blood vessels, representing ventriculo-arterial valves. The valve module is also used to represent connections between veins and atria, or atrial and ventricular septal defects. The valve module consists of a narrow orifice whose area varies over time during a cardiac cycle. Assuming unsteady, incompressible and non-viscous laminar flow, and the influence of gravity being neglected, the Bernoulli equation for unsteady flow can be written as,

$$I \cdot \frac{dq}{dt} + \frac{1}{2}\rho \cdot \left(v_{dist}(t)^2 - v_{prox}(t)^2\right) + \left(p_{dist}(t) - p_{prox}(t)\right) = 0 \qquad (1)$$

where ρ is blood density, I is the inertance of the valve, and dq/dt is the rate of change of blood flow across the valve. The blood flow velocities and pressures at the proximal and distal elements are $v_{prox}(t)$ and $p_{prox}(t)$, and $v_{dist}(t)$ and $p_{dist}(t)$, respectively (**Supplementary Figure 1**). By re-arranging **Eq. 1**, the pressure gradient ($\Delta p(t) = p_{prox}(t) - p_{dist}$) can be expressed as,

$$\Delta p(t) = I\frac{dq}{dt} + \frac{1}{2}\rho \cdot \left(v_{dist}(t)^2 - v_{prox}(t)^2\right) \qquad (2)$$

Since we assume that when blood flow passes a valve, there is no regain in pressure despite a decrease in velocity (i.e. energy is lost by means of friction or turbulence), **Eq. 2** can be re-arranged as,

$$\Delta p(t) = I \cdot \frac{dq_{valve}}{dt} + \frac{1}{2}\rho \cdot \begin{cases} v_{max}(t)^2 - v_{prox}(t)^2, & q_{valve}(t) \geq 0 \\ v_{dist}(t)^2 - v_{max}(t)^2, & q_{valve}(t) < 0 \end{cases} \qquad (3)$$

The pressure gradient in **Eq. 3** is the sum of inertial effects, i.e., blood acceleration/deceleration because of blood mass (**Eq. 3**, right hand side, first term) and Bernoulli pressure loss effects (**Eq. 3**, right hand side, second term). Blood flow, q_{valve}(t), across a valve is defined as forward flow ($q_{valve}(t) \geq 0$) when it travels from the proximal into the distal element, and backward flow ($q_{valve}(t) < 0$) in the opposite direction. In **Eq. 3**, the maximum velocity, $v_{max}(t)$, is:

$$v_{\max}(t) = max\{v_{prox}(t), v_{valve}(t), v_{dist}(t)\}. \qquad (4)$$

Flow velocities $v_{prox}(t)$, $v_{valve}(t)$ and $v_{dist}(t)$ are calculated as valve flow, $q_{valve}(t)$, divided by the cross-sectional area at the proximal element, valve and distal elements at time t, respectively. The effective orifice area (or cross-sectional area) of a valve at time t, $A_{valve}(t)$, is determined by the pressure gradient. When the valve is open, $A_{valve}(t) = A_{open}$, and when it is closed, $A_{valve}(t) = A_{leak}$. The valve opens rapidly when the pressure gradient is positive ($p_{dist}(t) < p_{prox}(t)$), allowing forward flow across the valve into the distal element. When the distal pressure is equal to the proximal pressure ($p_{dist}(t) = p_{prox}(t)$), the valve starts closing. In the closing state, the pressure gradient is negative ($p_{dist}(t) > p_{prox}(t)$), but a forward flow can briefly exist because of inertial effects (**Eq. 1**). A valve finally closes when the pressure gradient is negative and no forward flow remains. Note that in this study, a 'closed' valve allows retrograde flow to occur through the regurgitant orifice area as described in the main text, because A_{leak} can be non-zero.

The inertance of a tube $I = \alpha \frac{\rho l}{A}$, where l is the length of the tube and A is the cross sectional area. α is a constant reflecting the non-linearity of the flow profile. CircAdapt uses α = 3/2, representing a highly nonlinear flow through the valve (compare with α=1 for plug flow and α = 4/3 for Poiseuille flow). In CircAdapt, the inertance takes into account blood moving through the areas immediately proximal to the valve, and immediately distal to the valve (**Supplementary Figure 1**). Combining these effects gives a total expression for the inertance as

$$I = \frac{3}{2}\rho\left(\frac{l_{valve}}{A_{valve}} + \frac{1}{2}\left(\frac{1}{\sqrt{A_{prox}}} + \frac{1}{\sqrt{A_{dist}}}\right)\right) \quad (5)$$

Note, as stated before, that the valve module is used to connect any two cavities in the CircAdapt model where energy losses might occur, such as veins returning to the atria, or in case of an atrial or ventricular septal defect. In these cases, we define $A_{leak} = A_{open}$.

Flow across the systemic and pulmonary circulations

The CircAdapt model consists of a four-chamber heart connected to a closed loop cardiovascular system, with lumped pulmonary and systemic circulations (**Supplementary Figure 2, Panel A**). The systemic circulation is modelled as a vascular resistance connecting the aorta with the systemic veins. In CircAdapt, both the arterial and venous pressures vary with time, and the pressure difference

between the arteries and veins determines the flow across the systemic circulation at any point in time, *t*. The time-dependent flow across the systemic circulation $q_{sys}(t)$ is assumed to relate with time-dependent pressure drop $\Delta p_{sys}(\mathrm{t})$ as,

$$q_{sys}(t) = \frac{q_{sys,ref}}{\Delta p_{sys,ref}} \cdot \Delta p_{sys}(\mathrm{t}) \quad (6)$$

where $q_{sys,ref}$ is the reference circulating blood flow and $\Delta p_{sys,ref}$ is the corresponding reference systemic pressure drop. $\Delta p_{sys}(\mathrm{t}) = p_{sys,art}(t) - p_{sys,ven}(t)$ is the difference between the pressure in the systemic arteries ($p_{sys,art}(t)$) and the systemic veins ($p_{sys,ven}(t)$) at each time point. By Ohm's law, $\frac{q_{sys,ref}}{\Delta p_{sys,ref}}$ is the resistance of the systemic vasculature. In the CircAdapt model, $q_{sys,ref}$ is always held constant, but $\Delta p_{sys,ref}$ can be changed between cardiac cycles in the homeostatic control system described below. Hence, changing $\Delta p_{sys,ref}$ changes the systemic resistance in CircAdapt. Intuitively, $\Delta p_{sys,ref}$ can be seen as the pressure difference between the systemic arteries and systemic veins that would be required to generate a constant systemic flow of $q_{sys,ref}$. The relationship for the pulmonary circulation is similar to **Eq. 6**,

$$q_{pulm}(t) = \frac{q_{pulm,ref}}{\Delta p^2_{pulm,ref}} \cdot \Delta p_{pulm}(t)^2 \quad (7)$$

where $q_{pulm,ref}$ is the reference pulmonary circulating blood flow and $\Delta p_{pulm,ref}$ is the corresponding pulmonary pressure drop. The quadratic relationship in **Eq. 7** is based on measurements of pulmonary circulatory haemodynamics in dogs.[11] A description of the systemic and pulmonary circulation models, including the pressure-volume relationships in the major arteries and veins, can be found in Arts et al, Mech Res Commun 2011;42:15-21.

Pressure-flow regulation

In CircAdapt, homeostatic pressure-flow regulation is used to maintain a target cardiac output ($q_{sys,target}$) and target mean systemic arterial pressure (MAP_{target}). In the current study, $q_{sys,target}$ changes depending on the level of exercise. Note that $q_{sys,target}$ is not necessarily the same as $q_{sys,ref}$ in **Eq. 6** above. In CircAdapt, homeostatic pressure-flow regulation represents two physiological processes. Acutely, it represents the recruitment of pooled blood in the venous system into the circulating blood volume. In the longer term (for example when employed in simulations of heart failure, e.g.: Lumens et al, Circ Cardiovasc Imaging 2015;8:e003744), it represents the long-term action of the Renin-Angiotensin-Aldosterone system (RAAS) on fluid retention to maintain cardiac output. Both interpretations are

present in this study, with the former used in exercise and the latter used to maintain the baseline cardiac output.

When pressure-flow regulation is enabled, CircAdapt calculates at the end of each cardiac cycle the ratio between the current mean systemic arterial pressure over the cardiac cycle ($MAP_{current} = \overline{p_{sys,art}(t)}$) and the target mean aortic pressure (MAP_{target}) (**Supplementary Figure 2, red dot**). This ratio is then used to incrementally alter the systemic resistance through changes in $\Delta p_{sys,ref}$ (**Eq. 6**), with the process repeated over repeated cardiac cycles until $MAP_{current} = MAP_{target}$. In this study, a MAP_{target} of 92mmHg was used. After each cardiac cycle, the new value of the constant $\Delta p_{sys,ref}$, which determines the systemic vascular resistance during the next cardiac cycle (**Eq. 6**), is calculated using:

$$\Delta p_{sys,ref,new} = \left(\frac{MAP_{target}}{MAP_{current}}\right)^{\alpha} \cdot \left(\frac{q_{sys,current}}{q_{sys,target}}\right)^{\alpha} \Delta p_{sys,ref,old} \qquad (8)$$

Hence, the systemic vascular resistance will increase when MAP is too low, and decrease when systemic flow is too low. $\alpha < 1$ is a damping factor that prevents oscillatory behaviour. Note that the pulmonary resistance remains unchanged.

To represent RAAS and/or recruitment of pooled blood, the circulating blood volume alters with the systemic vascular resistance. These processes are implemented by injecting or removing volume per cardiac cycle into the cardiac system from the systemic vascular bed, i.e. by altering the flow at the arrow highlighted in **Supplementary Figure 2** (**Panel A, red arrow**). The flow across the systemic circulation $q(t)$ is calculated at each time point t in the cardiac cycle using **Eq. 6**. The flow entering the systemic veins $q_{ven}(t)$ at each time point is then adjusted, so that

$$q_{ven}(t) = \left(\frac{MAP_{target}}{MAP_{current}}\right)^{\alpha} q(t) \qquad (9)$$

Equivalently, **Eq. 9** can be seen as including an additional flow of magnitude $\left(\left(\frac{MAP_{target}}{MAP_{current}}\right)^{\alpha} - 1\right) q(t)$ into the flow exiting the systemic circulation into the systemic veins. Note that if $MAP_{target} > MAP_{current}$, then the additional flow is positive, analogous to recruitment of pooled blood into the circulation or fluid retention by RAAS. If $MAP_{current} > MAP_{target}$ then this flow is negative and removes blood from the circulation, analogous to blood pooling in the veins or fluid excretion through RAAS.

Simulating Exercise

The above method is used to simulate exercise by using an imposed cardiac output – heart rate relationship (**Supplemental Figure 3**). In this relationship, the heart rate is used to determine cycle length t_{Cycle}, which is an input to the model. In CircAdapt, cycle length determines the time period between onsets of right atrial contraction. The target cardiac output corresponding to that heart rate is set as $q_{sys,target}$ in **Eq. 8** above, with MAP_{target} left unchanged at 92mmHg. The system is then allowed to stabilize until MAP_{target} and $q_{sys,target}$ are reached.

To enable realistic simulation of exercise, the atrio-ventricular delay between right atrial activation and onset of ventricular activation (first activated segment in **Supplemental Figure 2**) has to shorten with decreasing cycle time, representing physiological PR interval shortening. CircAdapt sets the atrio-ventricular delay to be 0.1765× t_{Cycle}.

Duration of myocardial contraction also shortens as the heart rate increases (i.e, cycle time decreases). CircAdapt uses a phenomenological model of myocardial contraction, described in detail in the supplemental material of Walmsley et al, PLoS Comput Biol 2015;11:e1004284. The rise time (τ_R), decay time (τ_D) and contraction duration (T_A) all depend on the cycle length as follows,

$$\tau_R = T_R T_{Act} \tag{10}$$

$$\tau_D = T_D T_{Act} \tag{11}$$

$$T_A = (0.65 + 1.057\lambda_{si}) T_{Act} \tag{12}$$

Where T_D and T_R are constants, λ_{si} is the extension of the contractile element, and

$$T_{Act} = 0.1 t_{Cycle,rest} + 0.4 t_{Cycle}, \tag{13}$$

where $t_{Cycle,Rest}$ is the cycle time at rest.

Dyssynchronous Activation

Dyssynchrony is simulated using the MultiPatch method as described by Walmsley et al. PLoS Comput Biol 2015;11:e1004284, to which the reader is referred for methodological details. This method allows ventricular walls to be broken up into ‘patches’ of tissue and thereby simulate regional differences in function. Wall tension is assumed to be equal in all patches within a wall, but properties such as activation time can vary between patches, giving rise to differences in stresses and strains between patches. In the current study, the right ventricular free wall was broken up into five patches with equal

volumes. Only activation time differs between patches; myocardial intrinsic contractility and stiffness are not altered. The right ventricular free wall also interacts with the septum and LV free wall through the right ventricular attachment points, where force balance is enforced. The reader is referred to Lumens et al. Ann Biomed Eng 2009;37:2234-2255 for methodological details on ventricular interaction.

Simulation Code

The code for the CircAdapt model used in this study is free to download at www.circadapt.org. This study is based on the version previously published by Walmsley et al., PLoS Comput Biol 2015;11:e1004284.

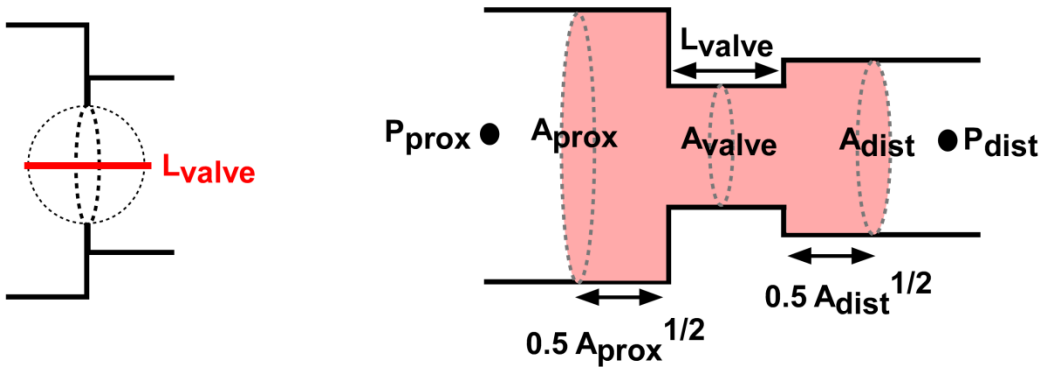

Figure S1: Definitions used in the text for the simulation of valvular function. The pink area indicates the total volume of blood considered in the inertance of the valve.

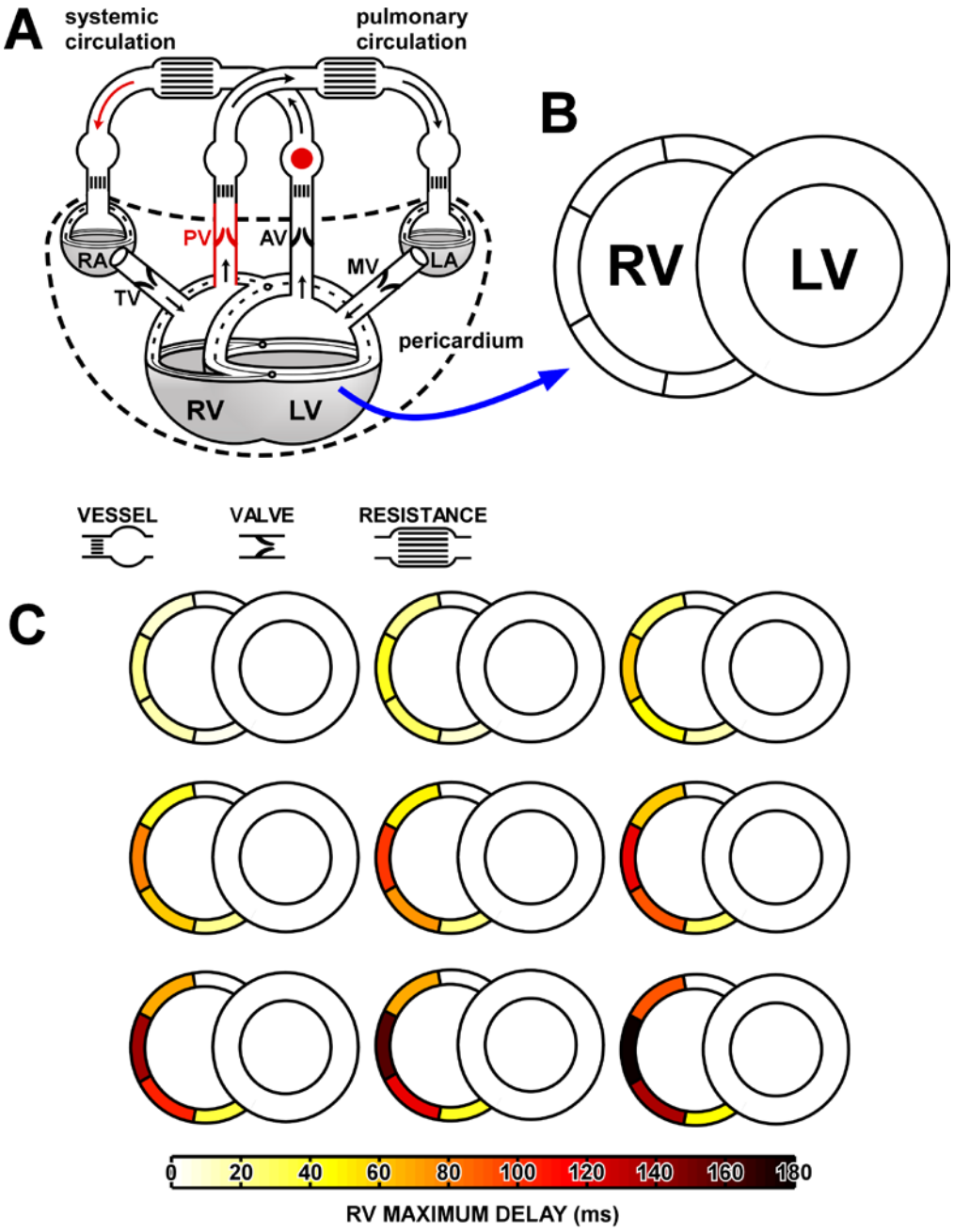

Figure S2: Panel A shows a schematic diagram of the CircAdapt model, modified from Lumens et al. Ann Biomed Eng. 2009;37(11):2234-55, with permission. Red has been used to highlight key parts of the model for this study referred to in the supplemental methods, being the pulmonary valve, pressure control in the aorta, and systemic venous return. **Panel B** shows a schematic of the ventricles in the synchronous case, with location in the model indicated by the blue arrow. Note that the LV is always synchronously activated in this study. **Panel C** shows the remaining nine activation patterns, with progressively increasing delay within the RV free wall. The colour bar indicates the magnitude of the delay in each segment. RV segments are activated at 0%, 25%, 50%, 75% and 100% of the latest RV activation time in each case.

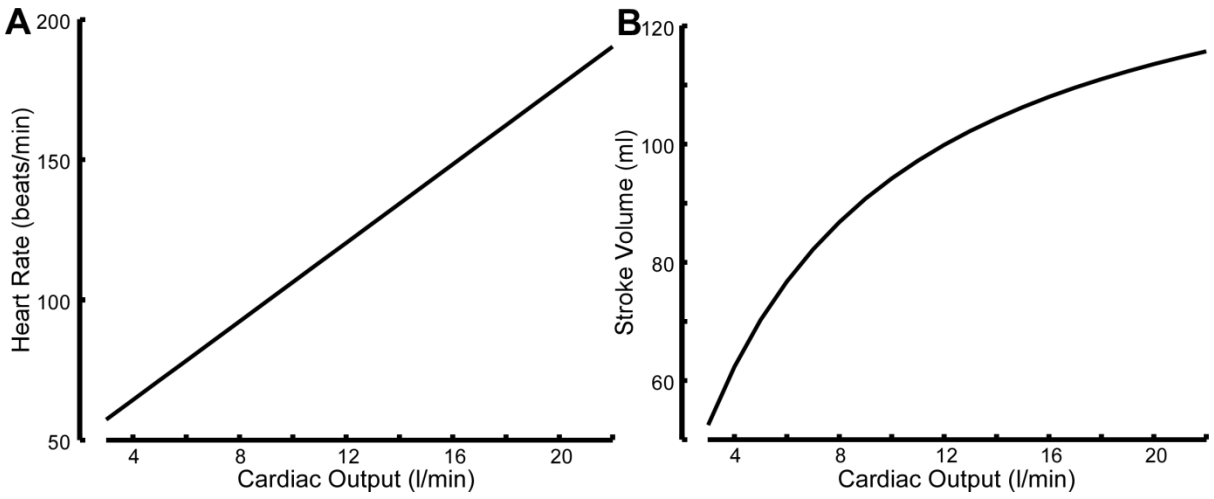

Figure S3: Heart rate – LV cardiac output relationship used in this study (**Panel A**). The corresponding stroke volume – cardiac output relationship is shown in **Panel B**. This relationship is based on linear interpolation of data recorded in healthy adults from WF Boron and EL Boulpaep, *Medical Physiology*, Elsevier Science 2003.

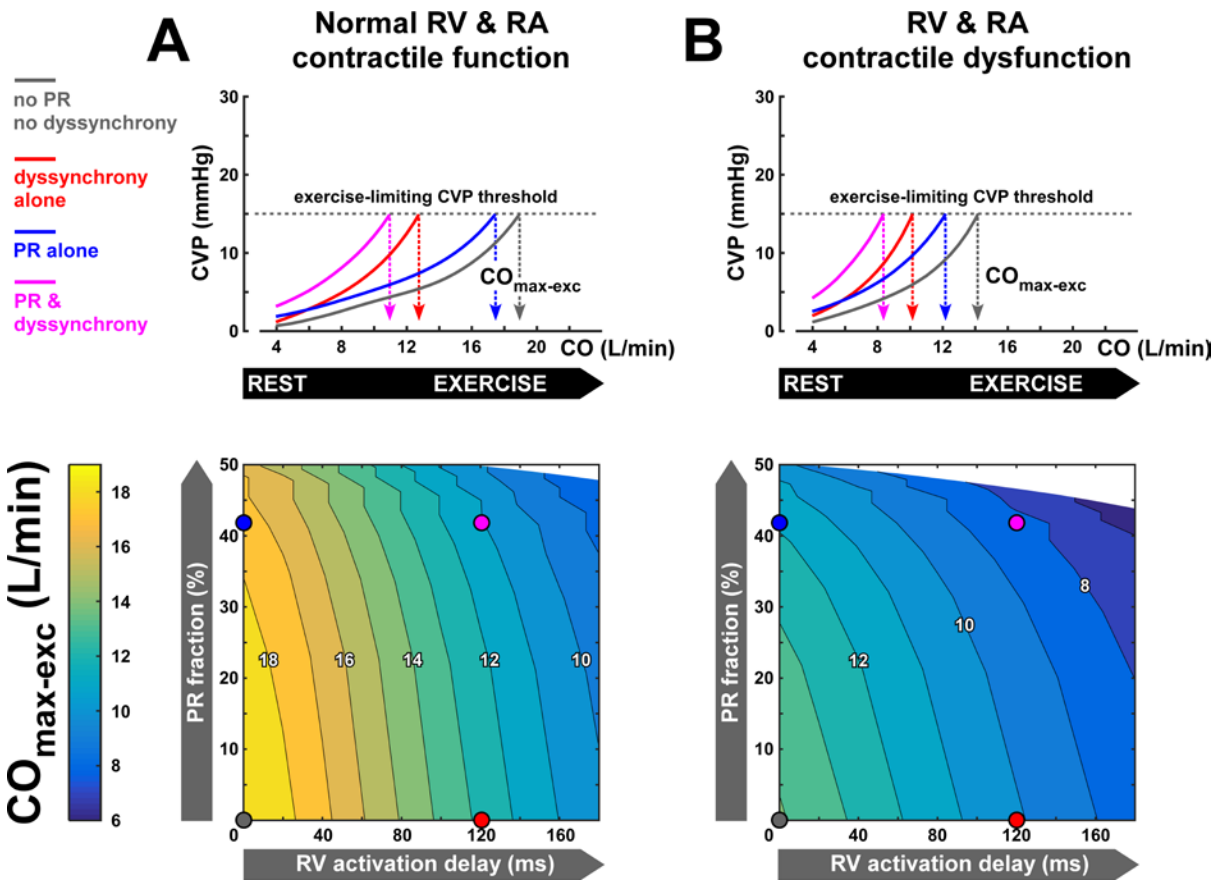

Figure S4: Exercise capacity (using 15 mmHg as the pressure threshold) as function of right ventricular (RV) dyssynchrony and pulmonary regurgitation (PR) in the virtual rTOF patient cohorts with normal (**panel A**) and decreased (**panel B**) contractile function of the RV and right atrial (RA) myocardium. The upper panels show how CVP rises with CO during exercise in four representative virtual rTOF patients. Those virtual patients are marked by circles in the heat plots showing continuous effects of RV dyssynchrony and PR on exercise capacity. Simulated exercise capacity is defined as the virtual patient's cardiac output ($CO_{max\text{-}exc}$) associated with the exercise-limiting central venous pressure (CVP) threshold. In general, RV dyssynchrony and contractile dysfunction are more limiting for exercise capacity than PR.

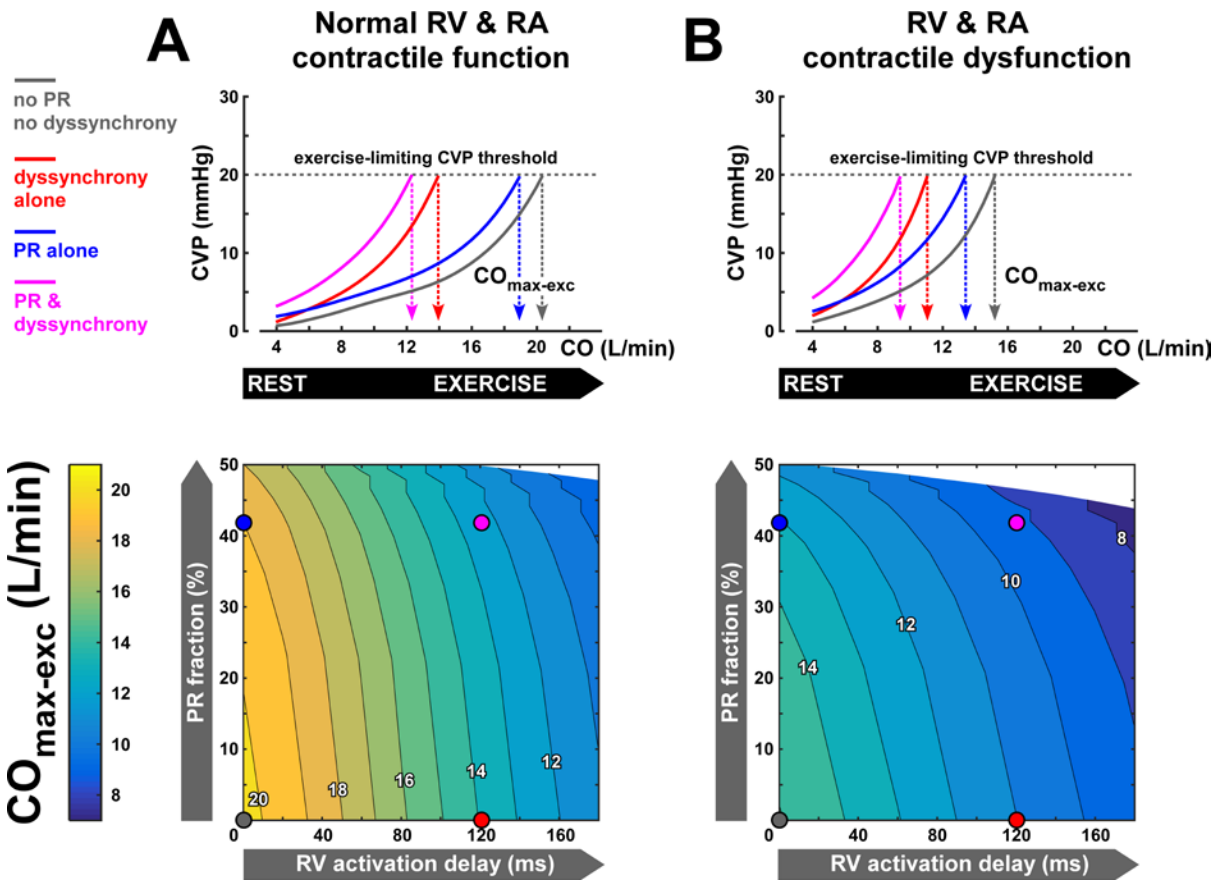

Figure S5: Exercise capacity (using 20 mmHg as the pressure threshold) as function of right ventricular (RV) dyssynchrony and pulmonary regurgitation (PR) in the virtual rTOF patient cohorts with normal (**panel A**) and decreased (**panel B**) contractile function of the RV and right atrial (RA) myocardium. The upper panels show how CVP rises with CO during exercise in four representative virtual rTOF patients. Those virtual patients are marked by circles in the heat plots showing continuous effects of RV dyssynchrony and PR on exercise capacity. Simulated exercise capacity is defined as the virtual patient's cardiac output ($CO_{max\text{-}exc}$) associated with the exercise-limiting central venous pressure (CVP) threshold. In general, RV dyssynchrony and contractile dysfunction are more limiting for exercise capacity than PR.